THE MACRO/MICRO MANIPULATOR: AN IMPROVED ARCHITECTURE FOR ROBOT CONTROL

Andre Sharon
Neville Hogan
David Hardt

Department of Mechanical Engineering
Massachusetts Institute of Technology
Cambridge, Massachusetts 02139

ABSTRACT

A macro/micro manipulator system, consisting of a large (macro) robot carrying a small (micro) high performance robot, is proposed as a means of enhancing the functionality of a manipulator. The objective of the research presented in this paper was to investigate the inherent features in dynamic performance of such a system, and to evaluate its feasibility.

The effect of a micromanipulator on the stability and performance of a robot system was investigated. It was found that a macro/micro manipulator is an inherently stable and well suited physical architecture for endpoint control.

A robust controller design based on physical equivalence and impedance matching is proposed. It is shown that both endpoint position and force control bandwidths higher than the structural frequencies of the robot can be achieved with minimal knowledge of the structure.

A five degree-of-freedom micromanipulator that can accelerate a 22 Kg mass at 45G's was designed, fabricated, and attached to an experimental one-axis robot. Using this system, a force control bandwidth of 60 Hz (32 times higher than the first structural mode of the robot) was achieved against and environment that is five times stiffer than the robot structure. An endpoint position control bandwidth of 28 Hz (15 times higher than the first structural mode of the robot) was also achieved. This can improve endpoint accuracy, reduce cycle-time, and enhance the robot's capability to successfully interact with a large class of environments.

IEEE Trans on Robotics and Automation Dec. 1988

I. INTRODUCTION

Commercially available robotic manipulators are neither accurate, responsive, nor well suited to interact with their environment. Lack of accuracy is caused primarily by unmeasured deflections of the robot structure or drive, and low actuator/servo resolution. Poor response time is attributed to low actuator power and control-related limitations. Interaction with the environment is hampered by the inability to accurately modulate the endpoint impedance of the robot.

Since the endpoint or tool position of a robot is derived through kinematic transformations based on measurements taken at each joint, the endpoint is in effect controlled in an open loop fashion. Any unpredictable behavior down-stream of the sensors (such as structural bending, thermal expansions, etc.) is not measured and hence cannot be corrected.

It is clear that the absolute endpoint or tool position can best be obtained by measurement of the endpoint rather than any other point on the robot. However, correction of small endpoint errors generally requires movement of several if not all the manipulator's actuators. Thus, each actuator must be capable of two very distinct tasks: it must provide high speed and good response for large range motion, while at the same time be capable of very accurate and quick fine motion. More importantly, direct measurement and control of the endpoint in conventional robot architectures results in non-collocated control (a dynamic system separating the actuator from the sensor) and has been shown to be inherently unstable [1]. This limits the achievable system bandwidth, detrimenting both response time and dynamic accuracy.

Non-collocation is a limiting factor in force control performance as well. The force sensor is commonly placed near the endpoint of the robot, while the actuators are located at the base of each link, resulting in non-collocated control. This problem often manifests itself as chatter, in which the robot repeatedly loses contact with the environment.

A macro/micro manipulator [2] system, consisting of a large (macro) robot carrying a small (micro) high performance robot, alleviates these problems by providing an in-

herently stable and well suited physical architecture for endpoint control. The macro-manipulator carries the micromanipulator to the vicinity of a task, where the inherent features of both the macro and micro robots are used in conjunction with endpoint sensing to achieve the desired goal (see Figure 1). Such a system can provide all the features of a small high precision robot for local operations, while at the same time retaining the versatility, speed, and work-space of a larger robot.

Intuitively, there are several advantages in the dynamic behavior that immediately stand out. First, the endpoint impedance of the robot can be modulated locally using the micromanipulator. This would enhance the system's capability to successfully interact with a wide range of environments.

Second, neglecting for a moment any control problems that may arise, a fast micormanipulator should be able to compensate for the settling time of the macromanipulator thus reducing cycle time, as well as for tracking errors encountered in following a prescribed path.

Third, the endpoint inertia of the robot is physically reduced, requiring less control effort in responding to varying conditions, such as an impact. The force transients generated during an impact are directly related to the inertia of the colliding members, and often occur too quickly to be actively controlled. When a macro/micro manipulator experiences an impact, it is the low inertia of the micromanipulator that is first seen at the interaction port, hence reducing the magnitude of the associated force transients. Thus, a smoother transition can be achieved between unconstrained and constrained motion, enabling a higher approach speed in contacting the environment.

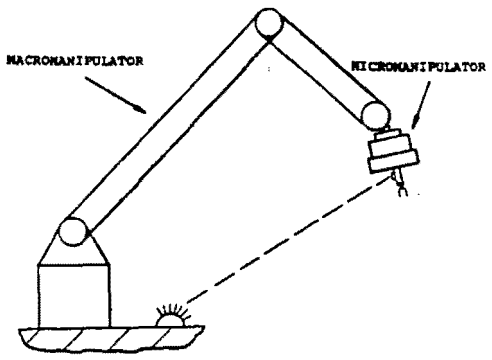

Figure 1. Macro/Micro Manipulator System.

Counter-intuitively, increasing the number of actuators (properly located) actually improves stability, and greatly reduces the control problem as will be shown in this paper.

One problem that immediately stands out, however, is that of endpoint measurement. In the most general sense, a system is needed that will measure not only the position of the endpoint in space, but also its orientation. Furthermore, the sampling rate of the measurement system must be very high since it will be used in the control loop. While progress is being made in this area, an adequate system does not yet exist. Nevertheless, there are many applications where the absolute position of the robot's endpoint is not required. Instead, its position relative to a work-piece, while interacting with it, is of primary importance. Since during this phase the robot is confined to a small area of the work-space, accurate position measurement is more readily achieved.

The concept of a macro/micro manipulator as a general means of improving a robot's controlled dynamic behavior has been investigated by the authors [2,3,4,5,6] and Cannon's group - more specifically Chiang [7], and Tilley and Cannon [8]. Several other researchers have also suggested the attachment of an actuator on the end of a robot for a specific purpose.

Hollis [9] developed a fine positioning device that can position a 100 gram load with a resolution of 0.5 microns. This is very useful in electronic component fabrication.

Van Brussel and Simmons [10], Cutkosky and Wright [11], Asakawa et al [12], and Kazerooni and Guo [13] developed active versions of the passive remote center compliance device (RCC) introduced by Whitney [14]

Salisbury [15] and Jacobsen et al [16] developed dexterous hands to be attached to manipulators. These hands are multi-fingered, and provide several additional degrees-of-freedom for intricate manipulation.

The authors have concentrated on the fundamental dynamic features of a macro/micro manipulator architecture, including the dynamic coupling between the micromanipulator and the macromanipulator structure. Such a configuration was found

to be inherently stable and well suited for endpoint control even at bandwidths higher than the structural frequencies of the robot.

This paper is divided into two major sections: unconstrained motion, in which there is minimal interaction between the robot and the environment (such as in spray painting, welding, etc.), and constrained motion in which the robot must be coupled to the environment (such as in grinding, drilling, etc.). In each case, stability and performance of a macro/micro manipulator is analyzed and compared to that of a conventional robot architecture. Experimental verification is provided.

II. UNCONSTRAINED MOTION

A. Stability

Consider the non-collocation problem exhibited by conventional robot architectures that are actuated at the base and whose endpoint is to be controlled. This is illustrated with a lumped parameter model of a one-axis robot structure shown in Figure 2a. The structure is actuated at the base (F) by feeding back the endpoint position measurement (X_n) . The actuation point is thus separated from the measurement point by some actuator dynamics, drive dynamics, structural dynamics, sensor dynamics, etc.

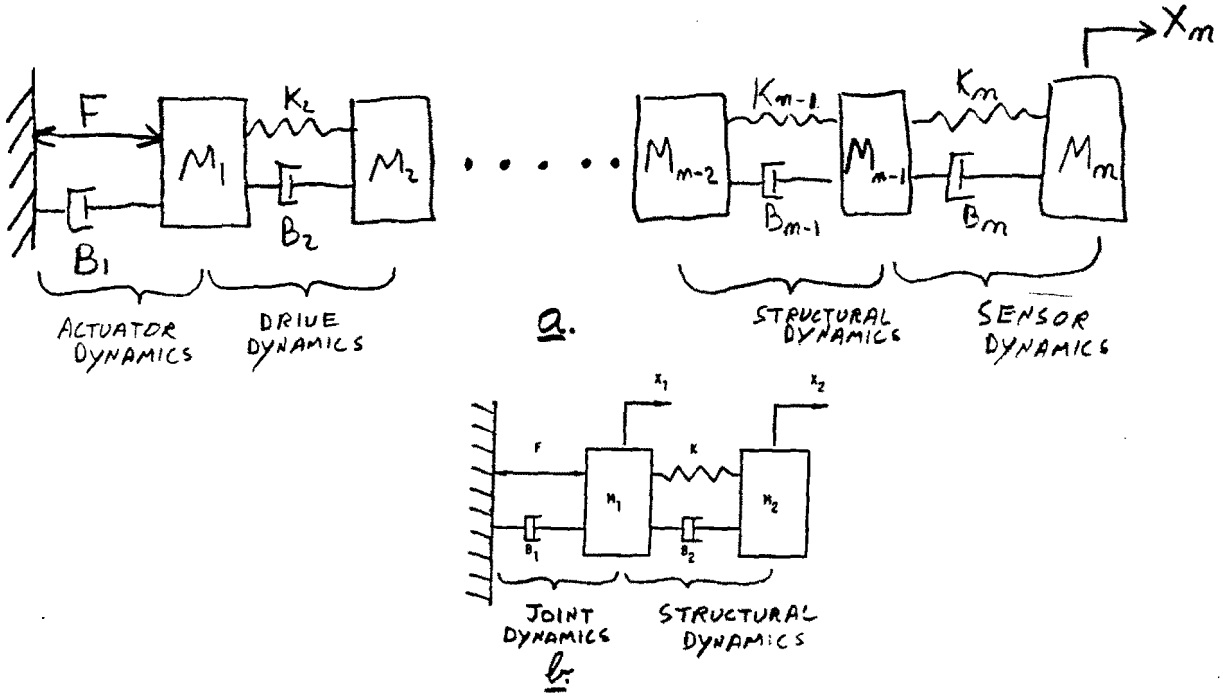

Figure 2. a. Model of a One-Axis Robot.
b. Simplified Model of a One-Axis Robot.

While such models have been investigated, it was found that more insight can be obtained by working with a simpler model (see Figure 2b) in which there is only one dynamic system separating the actuator from the sensor. This can be viewed as the critical dynamics between the actuation and measurement points. In this paper, a very flexible robot structure was investigated as a worst case scenario, and hence the structural dynamics were taken to be critical. Referring to the model of Figure 2b, the actuator force is denoted by F, along with some joint dynamics lumped into B_1 and M_1, while the structural dynamics are lumped into B_2,K, and M_2.

The equations of motion describing the system in Figure 2b are derived as:

$$\frac{d}{dt}\begin{bmatrix} X_1 \\ \dot{X}_1 \\ X_2 \\ \dot{X}_2 \end{bmatrix} = \begin{bmatrix} 0 & 1 & 0 & 0 \\ \frac{K}{M_1} & \frac{(B_1+B_2)}{M_1} & \frac{K}{M_1} & \frac{B_2}{M_1} \\ 0 & 0 & 0 & 1 \\ \frac{K}{M_2} & \frac{B_2}{M_2} & \frac{K}{M_2} & \frac{B_2}{M_2} \end{bmatrix} \begin{bmatrix} X_1 \\ \dot{X}_1 \\ X_2 \\ \dot{X}_2 \end{bmatrix} + \begin{bmatrix} 0 \\ \frac{1}{M_1} \\ 0 \\ 0 \end{bmatrix} [F] \qquad (EQ.\ 1)$$

and the transfer function between the endpoint position and actuator is determined to be:

$$\frac{X_2}{F} = \frac{K}{S[M_1M_2S^3 + (B_1M_2 + B_2M_2 + B_2M_1)S^2 + (B_1B_2 + KM_1 + KM_2)S + KB_1]} \qquad (EQ.\ 2)$$

It is seen in the transfer function above that the system is characterized by four poles and no zeros, giving rise to forty-five degree assymptotes as confirmed in the root locus of Figure 3. The parameter values used in this simulation are representative of the system described in reference 2, and are given below:

$M_1 = 0.0169$ lb • sec^2/*in*
$M_2 = 0.005$ lb • sec^2/*in*
$B_1 = 0.13$ lb • sec /*in*
$B_2 = 0.013$ lb • sec /*in*
$K = 24.0$ lb/in

As the gain is increased, two poles head towards the right-half plane and the system becomes unstable.

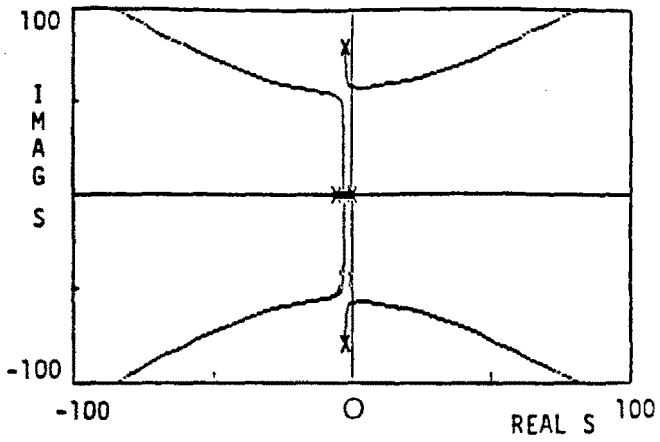

Figure 3. Root Locus of Endpoint Position Control ($F = -GX_2$) on a Robot.

Achieving stability in such a system is very difficult and there is a physical limitation on bandwidth due to the time required for a wave to travel the length of the structure [17].

Consider now a macro/micro manipulator in which there is an additional actuator attached to the end of the robot structure as shown in Figure 4a. The micromanipulator actuator is denoted by f along with some corresponding damping and inertia, B_3 and M_3. If the position of M_1 is regulated about zero with an infinitely stiff feedback loop, then the system in Figure 4a collapses to that of Figure 4b. This assumption reduces the order of the system, providing more physical insight. Furthermore, as will be explained in a later section, it is actually the worst case scenario.

The equations of motion characterizing this macro/micro manipulator system of Figure 4b are derived as:

$$\frac{d}{dt}\begin{bmatrix} X_2 \\ \dot{X}_2 \\ X_3 \\ \dot{X}_3 \end{bmatrix} = \begin{bmatrix} 0 & 1 & 0 & 0 \\ \frac{K}{M_2} & \frac{(B_2+B_3)}{M_2} & 0 & \frac{B_3}{M_2} \\ 0 & 0 & 0 & 1 \\ 0 & \frac{B_3}{M_3} & 0 & \frac{B_3}{M_3} \end{bmatrix}\begin{bmatrix} X_2 \\ \dot{X}_2 \\ X_3 \\ \dot{X}_3 \end{bmatrix} + \begin{bmatrix} 0 \\ \frac{1}{M_2} \\ 0 \\ \frac{1}{M_3} \end{bmatrix}[f] \qquad (EQ.\ 3)$$

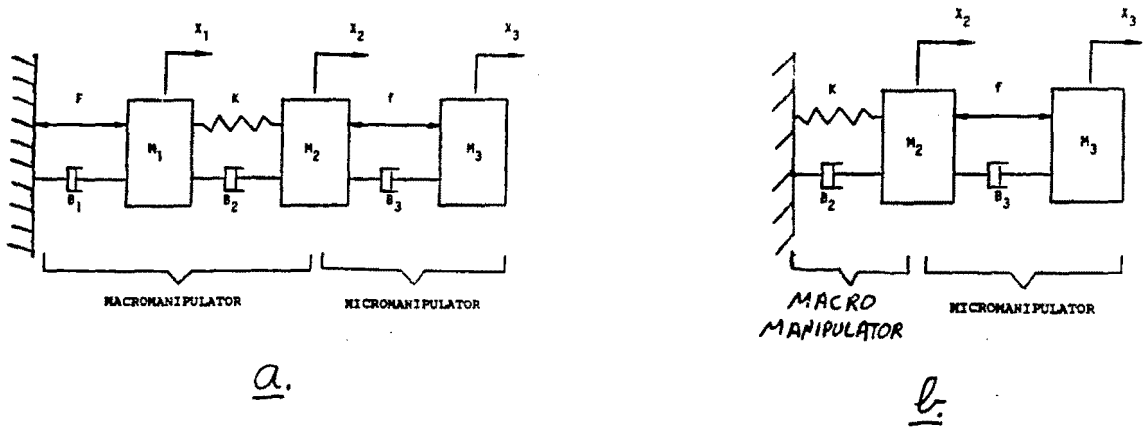

Figure 4. a. Model of a One-Axis Macro/Micro Manipulator.
b. Model of a One-Axis Macro/Micro Manipulator With an Infinitely Stiff Base Position Loop ($F = -\infty X_1$).

and the transfer function between X_3 and f is determined to be:

$$\frac{X_3}{f} = \frac{M_2S^2 + B_2S + K}{S[M_2M_3S^3 + (B_2M_3 + B_3[M_2 + M_3])S^2 + (B_2B_3 + KM_3)S + KB_3]} \qquad (EQ.\ 4)$$

Thus, the macro/micro manipulator architecture introduces two zeros in the numerator, giving rise to ninety degree assymptotes.

Using the following parameter values:

$$M_2 = 0.0169 \text{ lb} \bullet \text{sec}^2/in$$
$$M_3 = 0.005 \text{ lb} \bullet \text{sec}^2/in$$
$$B_2 = 0.013 \text{ lb} \bullet \text{sec}/in$$
$$B_3 = 0.13 \text{ lb} \bullet \text{sec}/in$$
$$K = 24.0 \text{ lb/in}$$

results in the root locus shown in Figure 5a. The parameters used in the simulation are representative of the macro/micro manipulator described in reference 2. It is seen in the root locus that while the complex poles become unstable en route to the zeros, the system is inherently stable at high frequencies. The Bode plot shown in Figure 5b also confirms that the system is stable at frequencies below as well as above the resonant frequency caused by the structural dynamics of the macromanipulator. It is only at

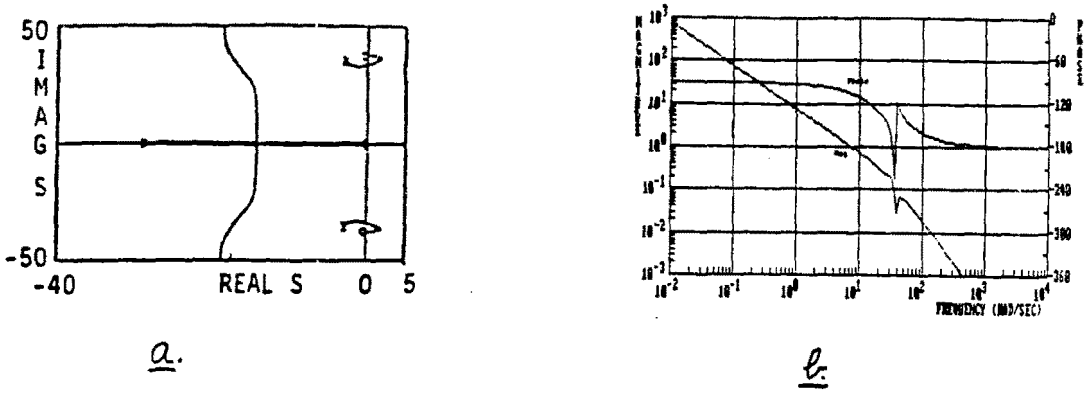

Figure 5. a. Root Locus ($f = -GX_3$) of a Macro/Micro Manipulator.
b. Open-Loop Bode Plot (X_3/f) of a Macro/Micro Manipulator.

frequencies close to the structural resonance of the macromanipulator that the system becomes unstable. Also, although the system is stable at high frequencies, the phase margin is very low. Thus, a controller must be devised that will stabilize the system in the neighborhood of the structural resonance of the macromanipulator, as well as provide a higher phase margin for improved performance.

One way of stabilizing the system is by attempting to cancel out the undesirable structural dynamics of the macromanipulator. The performance of such a controller, however, is highly dependent on a precise model of the system. While this may work in theory or even in tightly monitored laboratory situations, it is extremely difficult to achieve in real systems [2,17].

Examining the transfer function (EQ. 4) of the macro/micro manipulator, it is observed that if the endpoint inertia of the macromanipulator is much greater than the inertia of the micromanipulator ($M_2 >> M_3$) then the $B_3[M_2 + M_3]$ term in the denominator reduces to B_3M_2. Dividing the numerator by the denominator then results in the following transfer function:

$$\frac{X_3}{f} = \frac{1}{M_3S^2 + B_3S} \qquad (EQ.\ 5)$$

in which the dynamics of the macromanipulator are eliminated. The resulting system is equivalent to a micromanipulator attached to ground and is stable at all frequencies. While this condition my be feasible in systems designed for very light payloads, in the general case, the endpoint inertia of the macromanipulator is not sufficiently larger than the inertia of the micromanipulator, especially if the mass of the load is lumped with that of the micromanipulator.

Another way of stabilizing the system is by increasing the structural damping (B_2) of the macromanipulator. This biases the pole-zero pairs to the left, avoiding instability. Increasing structural damping, however, is physically difficult to achieve, although not impossible [18].

A more realizable and robust approach to stabilizing the system is through endpoint velocity feedback. If the control law prescribed to the micromanipulator is of the form:

$$f = -G_1 X_3 + G_2 \dot{X}_3$$

then as long is G_2 is taken to be large enough, the system becomes stable over the entire frequency range, as is shown in the Bode plot of Figure 6 where G_2 was taken to be 4. Feeding back $\dot{X}_3$ biases the root locus to the left, such that the complex poles no longer cross over to the right-half plane on the way to the complex zeros. Besides stabilizing the system, feedback of $\dot{X}_3$ also raises the phase margin at high frequencies.

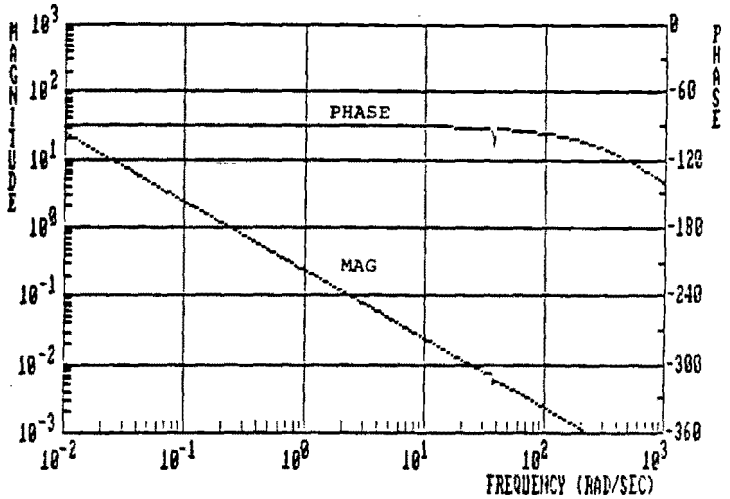

Figure 6. Open-Loop Bode Plot (X_3/f) of a Macro/MicroManipulator With Endpoint Velocity Feedback.

Note that feeding back $\dot{X}_3$ (endpoint velocity relative to ground) is not equivalent to raising the micromanipulator damping (B_3) . Increasing B_3 does not stabilize the system.

While the models used in this analysis are simple, they provide a great deal of physical insight. The important system characteristics are clearly brought out. The primary concern in regulating the endpoint position of a macro/micro manipulator is the dynamic coupling between the macro and micro manipulators. More specifically, it is the narrow instability band caused by the structural resonances of the macromanipulator, and the low phase margin at high frequencies. Both of these issues are observed in the Bode plots and root loci obtained from these simple models, and hence are accounted for.

In fact, when the control law proposed above is incorporated in a higher order model (including servo-valve dynamics and fluid compressibility) specifically developed for the hydraulic macro/micro manipulator described in reference 2, the resulting response is very similar to that obtained with the simple models. Furthermore, experimentation with a real macro/micro manipulator confirms the validity of these models.

The advantage, on the other hand, of using simple, yet adequate models, is that a better physical insight to the system is obtained. Having this insight led to the proposal of a simple, yet robust controller that was not at all evident when working with the higher order models.

B. Enhancement of Dynamic Accuracy and Cycle-Time Reduction

The time taken by a robot to converge onto its final goal, once that goal is fed to the servo, is governed primarily its servo settling time. This may have a significant effect on cycle time, especially if there are many short moves that are very common in robotic applications.

Settling time is influenced by many factors. These include: inertia, actuator power, control strategy, etc. It is further limited by the structural resonance of the robot, as was pointed out in the previous section.

A fast micromanipulator attached to the end of a macromanipulator can compensate for this servo settling time by locking in on the target, thus maintaining the endpoint position in the desired location while the macromanipulator is settling. This would reduce the total cycle-time since the next move command can be issued before the macromanipulator completes its previous move.

A micromanipulator can also compensate for the tracking errors encountered in following a prescribed path in space. When a robot is commanded to follow a geometric path at a given velocity profile, each of its joints may have to respond with a different velocity and acceleration in order to maintain the endpoint on the desired trajectory. In fact, one or more of the joints may have to respond with an infinite acceleration to keep the endpoint from deviating from the the desired path. An example of this phenomenon is observed when a robot tries to go around a sharp corner with a constant speed, thus having to instantaneously stop some of its joints, while instantaneously accelerating others. This is a major problem in applications such as seam welding, seam caulking, spray painting, etc., where quality depends not only on positioning accuracy, but also on maintaining a prescribed speed.

As described previously, however, a robot's response bandwidth is physically limited. If, on the other hand, a high-bandwidth micromanipulator is attached to the end of the robot, it can compensate for the tracking errors encountered.

In evaluating this claim, a two-axis macro/micro manipulator model was analyzed. The reason for the two axes is to enable tracking of an arbitrary path along a given plane, and also to see if the conclusions derived from the one-axis model would apply to more degrees of freedom. In order to focus on the issues relevant to the introduction of the micromanipulator, the kinematics of the system were kept as simple as possible. Thus, translational degrees of freedom were chosen for both the macro and micro manipulators. However, in order to introduce dynamic coupling between the degrees of freedom, the micromanipulator axes were oriented at a forty-five degree angle from those of the macromanipulator (see Figure 7). The controller developed for the single-axis case was applied independently to each axis. The bandwidth of the macromanipulator

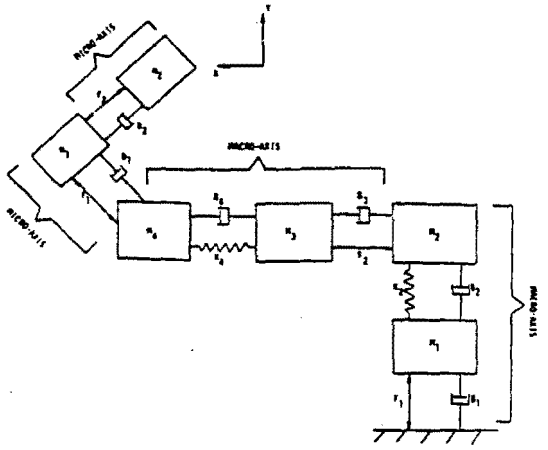

Figure 7. Model of Two-Axis Macro/Micro Manipulator.

was kept at about 4 Hz, while a 50 Hz bandwidth was taken for the micromanipulator. This is twice as high as the macromanipulator's structural frequency which was taken to be 25 Hz. The micromanipulator's travel was limited to 0.1 inches relative to the macromanipualtor.

In order to characterize the tracking performance of such a macro/micro manipulator, the system was commanded to track the perimeter of a square at a constant speed. The improvement in tracking with regard to both position and speed is simulated in Figure 8. The performance is greatly enhanced in both respects, but is most evident in the speed profile. Thus, a macro/micro manipulator enhances tracking performance, and consequently reduces cycle-time by maintaining accuracy at higher speeds.

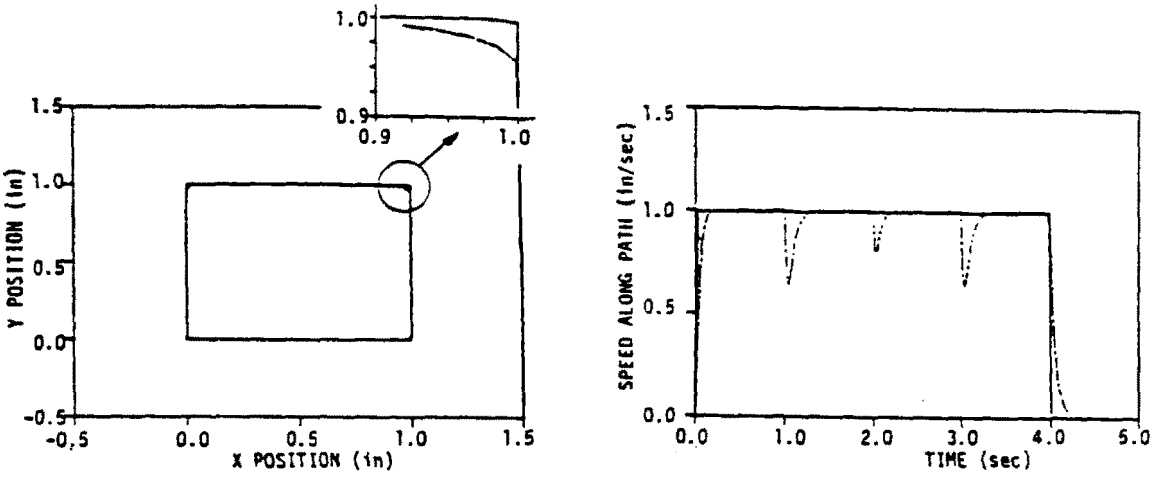

_____ Response of Macro/Micro Manipulator
_ _ _ _ Response of Conventional Robot

Figure 8. Comparison Between a Macro/Micro Manipulator and a Conventional Robot in Tracking the Perimeter of a Square.

III. CONSTRAINED MOTION

Many potential robot applications require the manipulator to be mechanically coupled to other objects during some phase of the operation. If the operation performed during the coupled phase results in either motion with no resisting forces or vice versa along any one axis, then there is no dynamic interaction, along that axis, between the robot and the object it is coupled to. An example of this would be a robot washing a window. There is negligible motion in the normal direction (assuming the glass does not break) while there is is negligible resisting force in the tangential direction (assuming low friction). It is thus sufficient to regulate force in the normal direction and position in the tangential direction [19]. Both the position controller and the force controller therefore attempt to track a desired input. A higher controller bandwidth thus results in better tracking ability.

In general, however, there are cases in which there is a net power transfer between the robot and its environment. These include grinding, drilling, engraving, metal bending, etc. The dynamic interaction is clearly not negligible and force or position control alone no longer suffices. Instead, the dynamic interaction between the robot and the environment must be controlled. Impedance Control has been proposed as a unified approach to this problem [20]

A general impedance consists of at least a stiffness, a damping, and an inertia component. Force feedback is a means of modulating the apparent impedance and especially the inertia component [21]. Positive force feedback approximates an increased apparent inertia, while negative force feedback approximates a decreased apparent inertia. A high inertia tends to keep the robot on its planned path regardless of the encountered motion constraints (high dynamic disturbance rejection). A low inertia tends to minimize interface forces by allowing the robot to quickly accept any motion dictated by environment (low dynamic disturbance rejection). In this perspective, force feedback is incorporated in order to change the apparent dynamics of a system, and not necessarily to track a desired force input.

Thus, whether for modulating impedance purposes, or for interface force regulation, high bandwidth negative force feedback is desirable. However, as will be seen in the next section, it is very difficult to achieve using conventional robot architectures.

A. Problems in Force Control

The force control problem has plagued researchers for many years. Four major causes, in the authors' view, are listed below. Immediately following is their description.

I. Instability caused by non-collocated actuators and sensor.

II. Initial impact.

III. Low interface damping.

IV. Actuator and/or drive non-linearities

The Non-collocation Problem

In order to regulate tip forces or modulate the endpoint impedance of a robot, the force sensor used in force feedback would yield the most accurate information when placed at the tip or endpoint of the robot. The actuators, however, are located at the base of the links. This gives rise to a situation of non-collocated control, leading to instability at high bandwidths primarily because of the interaction between sensor dynamics and the structural dynamics of the robot [21,22,23,24].

Consider the one-axis manipulator modeled in Figure 2b, this time coupled to the environment through a force transducer (K_t, B_t) as shown in Figure 9a. It is desired to control the interface force F_t (force in spring K_t) in a closed loop fashion ($F = -GF_t$). Deriving the equations of motion (see reference 6) of this system and using the following parameter values:

$$M_1 = 0.0169 \text{ lb} \bullet \text{sec}^2/in$$
$$M_2 = 0.005 \text{ lb} \bullet \text{sec}^2/in$$
$$B_1 = 0.13 \text{ lb} \bullet \text{sec}/in$$
$$B_2 = 0.013 \text{ lb} \bullet \text{sec}/in$$
$$K = 24 \text{ lb/in}$$
$$K_t = 150 \text{ lb/in}$$
$$B_t = 0.16 \text{ lb} \bullet \text{sec}/in$$

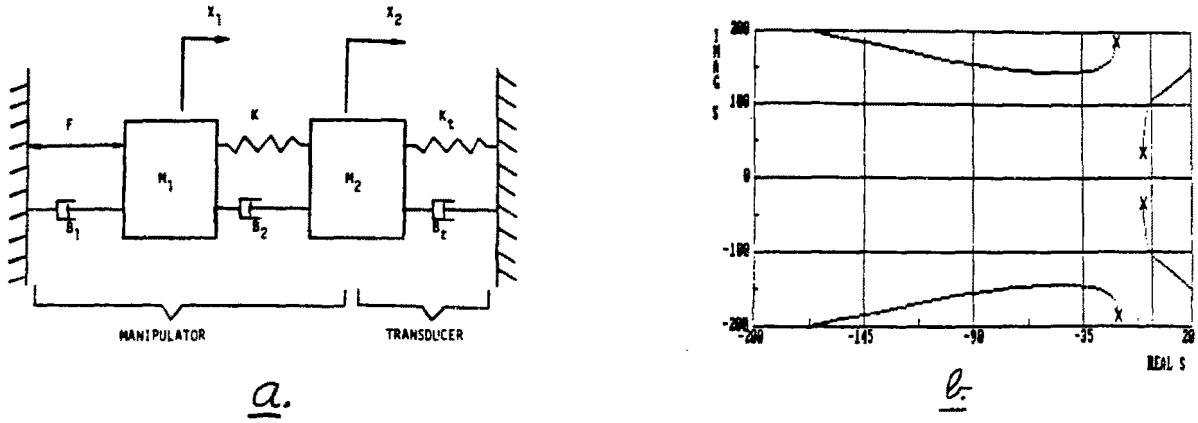

Figure 9. a. Model of a One-Axis Conventional Manipulator Coupled to a Rigid Environment.
b. Root Locus of Force Control ($F = -GF_t$) on a Conventional Manipulator.

results in the root locus plot shown in Figure 9b. The parameter values used here are representative of the system described in reference 2. The transducer parameter values were assumed to be those of a low-quality force transducer.

Examining the root locus in Figure 9b, it is seen that instability quickly results as the gain is increased. This is caused by the fact that the actuator and force transducer are not collocated, resulting in an interaction between the transducer dynamics and the structural dynamics of the manipulator. This problem can be somewhat alleviated by selecting a transducer significantly softer than the structural stiffness of the manipulator [22,23], or significantly stiffer [21]. Nevertheless, the system is inherently unstable at high bandwidths.

The Initial Impact Problem

When a robot first comes in contact with the environment, an impact occurs if the normal approach velocity differential between the robot and the environment is non-zero. This often causes the robot to bounce off the surface one or more times, and may lead to uncontrollable chatter. The force generated by an impact with a rigid environment is experienced too quickly to be controlled by the actuator. In fact, it would probably be best if the controller was disabled until the impact was over, avoiding a delayed, counter-productive reaction.

The impact force is a function of the interface characteristics between the robot and the environment. It is also a function of the approach velocity and the effective

endpoint inertia of the robot. If the interface characteristics and the approach velocity cannot be altered for a given application, the impact force can be reduced by decreasing the endpoint inertia of the robot.

The Low Interface Damping Problem

Many environments that a robot must interact with, such as metallic ones, are rigid and very lightly damped. This gives rise to oscillatory behavior even if stability is achieved. Although in principle endpoint velocity feedback relative to ground would increase the damping, it is very difficult to achieve in practice. The reason for this is that when a robot is in contact with a rigid environment, the resulting motion is generally below the resolution of the velocity transducer.

One way of increasing the effective damping ratio is by physically increasing the environmental or interface damping. This may or may not be feasible, depending on the particular application. An alternative way of increasing the effective damping ratio is by reducing the endpoint inertia of the robot, since the effective damping ratio is generally inversely proportional to the square root of the inertia.

The Actuator/Drive Non-linearity Problem

No real actuators behave like ideal torque sources. They all exhibit some degree of non-linearity such as dead-band, resolution limitations, ripple, etc. If a robot is commanded to exert a certain desired force on a rigid environment, chatter can occur if that desired force is within the range of the actuator's uncontrollable non-linearities or noise. This is independent of the non-collocation problem previously discussed.

The problem of uncontrollable actuator non-linearities or noise is even more detrimental in actuators that behave more like flow sources than torque sources. Examples are motors with high reduction transmission (non-backdrivable) and hydraulics. These actuators attempt to control force through position. In other words, if it is desired to apply a force F on an environment with a stiffness K, then the robot is displaced F/K "into" the environment. Thus, the actuator positioning "noise" is amplified by a factor

K, resulting in very large uncontrollable forces during interaction with stiff environments ($F = KX$). This effect can be reduced by using a soft interface (small K) between the robot and the environment.

Thus, since most commercial robots posses non-backdrivable actuator-transmission systems that behave like flow sources, it has often been stated that in order to achieve stability, the interface stiffness must be made low. While this alleviates the problem of actuator-drive imperfections, it does not solve the non-collocation problem. Hence, low interface stiffness yields stability, but only at low bandwidths. This is illustrated in Table 1 which lists the force control performance (in terms of bandwidth) achieved by others using base actuation - endpoint sensing. The list is by no means exhaustive, since reported results are often not quantified in terms of response time or bandwidth. It is seen that performance levels achieved on commercial robots are not very high. The non-collocation problem still limits achievable bandwidth, regardless of the interface characteristics. Table 1 also lists some of the achievements in force control using specially designed apparatus. These apparatus generally consist of high performance motors that resemble ideal torque sources, and very short and stiff structural members to reduce the non-collocation problem.

Hence, high performance force control can be achieved with the proper hardware. Use of short links, however, may often not be a practical solution, especially if dexterity is required.

RESEARCHERS	BANDWIDTH *
Whitney (1976)	2-3 Hz
Raibert and Craig (1981)	2-3 Hz
Khatib and Burdick (1986)	2-3 Hz
Maples and Becker (1986)	2-3 Hz
a.	
An (1986)	20 Hz
Youcef-Toumi and Negano (1987)	15 Hz
Kazerooni (1988)	20 Hz
b.	

* Estimated from reported step force responses when bandwidth was not explicetely given.

Table 1. Reported Achievements in Force Control Using Base Actuation - Endpoint Sensing.
a. Implementations on Commercial Robots.
b. Implementations on High Performance Apparatus.

A macro/micro manipulator is beneficial in alleviating the problems of force control described above. The effect of initial impact is reduced since the endpoint inertia (that of the micromanipulator) is very low. The effective endpoint damping ratio is increased because the endpoint inertia is lower. The problem of actuator-drive imperfections is also alleviated since it is generally easier to achieve a micro-actuator that resembles an ideal torque source, than one that must provide a large range of motion as well. Finally, as will be shown in the next section, a macro/micro manipulator alleviates the problem of non-collocated actuators and sensor exhibited by conventional robot architectures.

B. Stability of a Macro/Micro Manipulator Under Force Control

Consider the macro/micro manipulator modeled in Figure 4a, this time coupled to a rigid environment through a force transducer (see Figure 10). It is desired to regulate the interface force F_t (force is spring K_t) in a closed loop fashion. First it is investigated how the micromanipulator (f) alone can regulate the interface force, while the macro-manipulator actuator (F) is used to regulate the position of the macromanipulator about zero ($F = -GX_1$) . Then, it will be shown how the macromanipulator can be used in conjunction with the micromanipulator to better regulate interface forces.

Deriving the equation of motion describing the the system in Figure 10 (see reference 6), and using the following parameter values:

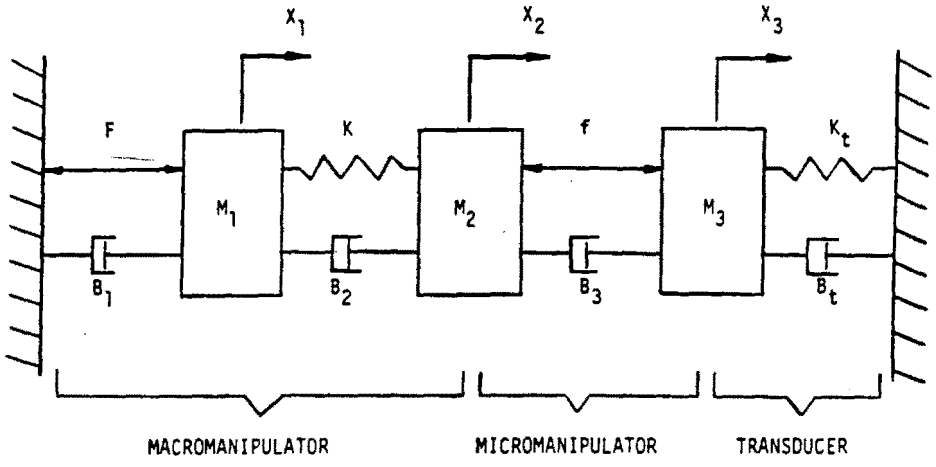

Figure 10. Model of a One-Axis Macro/Micro Manipulator Coupled to a Rigid Environment.

$M_1 = 0.0169$ lb • sec^2/*in*
$M_2 = 0.0169$ lb • sec^2/*in*
$B_1 = 0.13$ lb • sec /*in*
$B_2 = 0.013$ lb • sec /*in*
$K = 24$ lb/in
$K_t = 150$ lb/in
$B_t = 0.16$ lb • sec /*in*
$B_3 = 0.13$ lb • sec /*in*
$M_3 = 0.005$ lb • sec^2/*in*

results in the Bode plot of Figure 11 and root locus of Figure 12. The parameter values used here are representative of the macro/micro manipulator system described in reference 2.

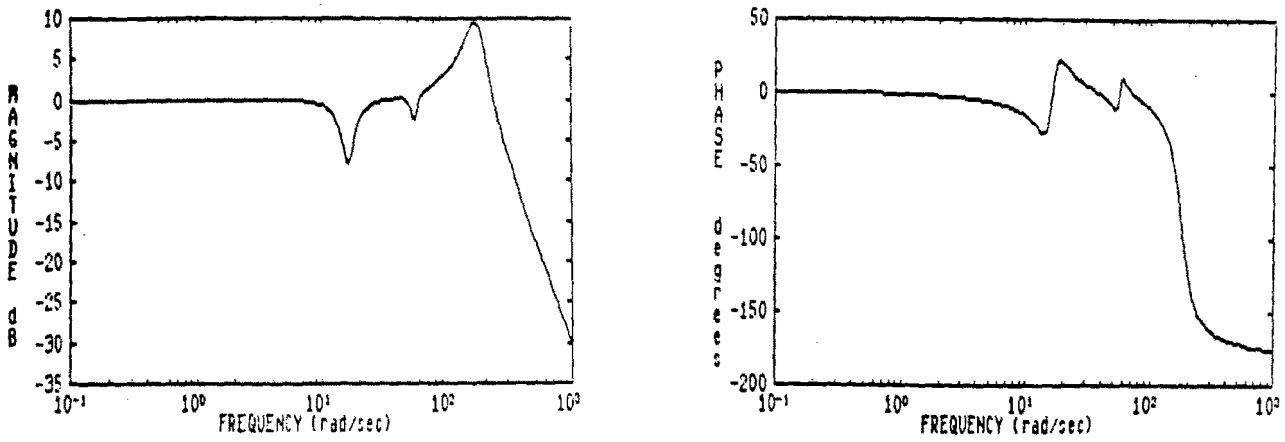

Figure 11. Open-Loop Bode Plot of Force Control (F_t/f) on a Macro/Micro Manipulator.

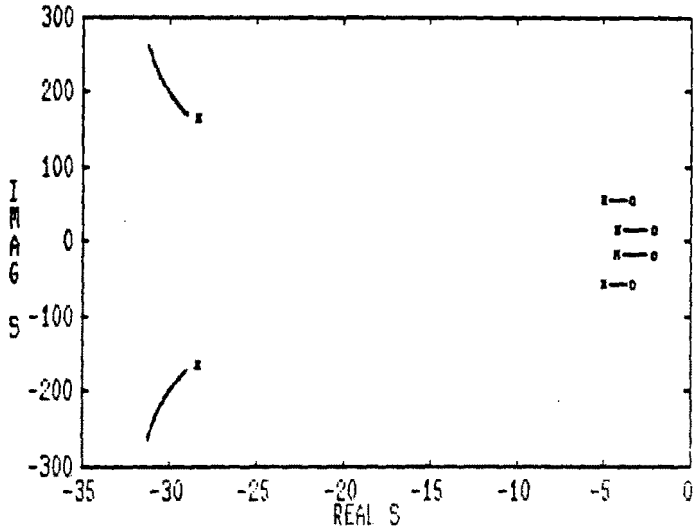

Figure 12. Root Locus of Force Control ($f = -GF_t$) on a Macro/Micro Manipulator.

Once again, the transducer parameter values were assumed to be those of a low-quality force transducer.

It is seen in both the Bode plot and root locus that the system remains stable at all frequencies, although there is some anti-resonance caused by the structural dynamics of the macromanipulator. Nevertheless, the analysis shows that a macro/micro manipulator system is an inherently stable physical configuration for high bandwidth force control. This is in contrast to conventional robot architectures that are inherently unstable at high bandwidth force control as was illustrated in Figure 9.

While simple, proportional negative force feedback implemented on the micromanipulator ($f = -GF_t$) proves to be stable, performance could be further improved. The observed anti-resonance caused by the structural dynamics of the macromanipulator must be addressed.

Controller Design

Designing a simple, yet robust controller based on the Bode plot and root locus of Figures 11 and 12 is very difficult. While the S-plane provides a great deal of information about stability, natural frequencies, etc., physical insight is lost. After all, if the control action is neglected for a moment, the model of the macro/micro manipulator in Figure 10 represents a physical system composed of masses, springs, and dampers. Furthermore, the concept of physical equivalence [20] suggests that for every controlled physical system there exists a purely (no control) physical system whose dynamic behavior is identical. Also, no control action can make a physical system behave like a non-physical system. Thus, a controlled physical system is a physical system as well. This enables us to design a controller in the physical domain.

Design in the Physical Domain [6,25] has been proposed as a means of integrating control systems design with mechanical systems design, by preserving physical insight, and providing some guidance in designing the proper physical architecture for a given task. This approach attempts to abstract to the physical system level, facilitating separation of design and implementation issues. Feedback is only introduced as means of

implementing some physical design requirements, such as increasing inertia, reducing stiffness, etc. A more complete description of this approach can be found in references 6 and 25. In this section, it shown how Design in the Physical Domain was used to develop a robust controller for the macro/micro manipulator.

Examination of the macro/micro manipulator model of Figure 10 reveals why the macromanipulator's structural dynamics are excited. Since there is very little dissipation capability in the structure (B_2 is very small), much of the energy transferred from the micromanipulator to the macromanipulator is reflected back through the structure, exciting structural modes. One way of alleviating this problem is to increase the structural damping (B_2). As was stated earlier, however, this is very difficult to achieve.

Another means of enhancing the capability to dissipate energy transferred by the micromanipulator to the macromanipulator is by increasing B_1 . However, arbitrarily increasing B_1 may not help. For example, in the limit as B_1 is raised to infinity, M_1 becomes a ground, and no energy is dissipated through B_1 . There should be, however, some value of B_1, between zero and infinity, that maximizes dissipation.

If the macromanipulator structure is viewed as a mechanical transmission line, where the micromanipulator is the source input and B_1 is the load, then the energy transferred from the source to the load can be maximized if the load's impedance is matched to the characteristic impedance of the transmission line [5]. This is known as impedance matching [26].

The characteristic impedance of a uniform, non-dissipative transmission line is given [26] as:

$$Z_o = \sqrt{\frac{L_o}{C_o}} \qquad (EQ.\ 6)$$

where L_o is the inductance per unit length and C_o is the capacitance per unit length. The reflection coefficient (R_l), quantifying the ratio of wave reflection back to the source is given [26] as:

$$R_l = \frac{Z_o - Z_L}{Z_o + Z_L} \qquad (EQ.\ 7)$$

where Z_L is the impedance of the load. Note that if the impedance of the load is matched to the characteristic impedance of the line ($Z_L = Z_o$) , R_f becomes zero and there is no reflection. In other words, all the energy input by the source is absorbed by the load. Such impedance matching tends to make a finite length transmission line appear to be infinitely long, eliminating reflection, and hence structural excitation. If Z_L is zero or infinity, then there is no energy absorbed by the load, since the load experiences flow with no effort or effort with no flow, respectively. This applies to the unconstrained case as well, and is the reason why an infinitely stiff position loop implemented on the macromanipulator actuator was said to be the worst case scenario.

Taking the mechanical equivalence yields of equation 6 yields:

$$Z_o = \sqrt{MK} \qquad (EQ.\ 8)$$

for the characteristic impedance of a non-dissipative mechanical transmission line. Thus, if the structural damping is neglected, the characteristic impedance of the macromanipulator structure can be approximated as:

$$Z_o = \sqrt{(M_1 + M_2)K} \qquad (EQ.\ 9)$$

If we set the value of B_1 equal to the characteristic impedance (Z_o), most of the energy transferred to the macromanipulator structure would be dissipated through B_1 , reducing the amount of reflection and hence structural modes excitation (see Figure 13). It is observed that the anti-resonance exhibited in the Bode plot of Figure 11 is greatly diminished.

Note that no where in the design process was feedback used. The entire design was performed at the physical system level (in terms of physical elements) using the vast knowledge of Physical Systems Theory. Feedback will be used as a one means of implementing this design.

The value of B_1 can be modulated by actually placing a mechanical damper on the joint axis, or through control action. Modulating B_1 through control action is easily

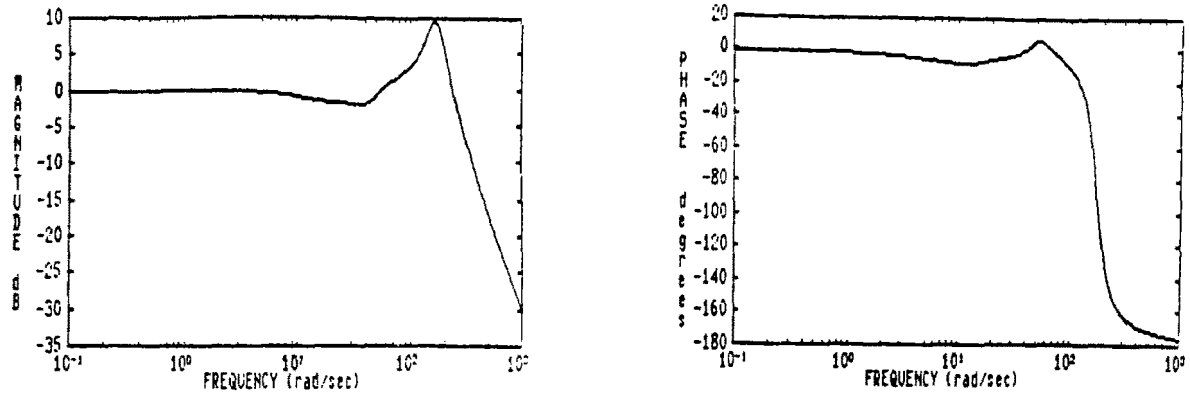

Figure 13. Open-Loop Bode Plot of Force Control (F_t/f) on a Macro/Micro Manipulator With Base Damping (B_1) Chosen Through Impedance Matching.

achieved since there already exists an actuator (F) between ground and M_1. The control law for the actuator would simply be:

$$F = G\dot{X}_1$$

Once the effect of the structural dynamics is alleviated, the micromanipulator can treat the macromanipulator as a low frequency disturbance, and high bandwidth force control can be achieved through proportional feedback:

$$f = -GF_t$$

Thus, a control action by the macromanipulator of the form:

$$F = -G_1X_1 + G_2\dot{X}_1$$

along with a control action by the micromanipulator of the form:

$$f = -G_3F_t$$

is sufficient to achieve force regulation at bandwidths much higher than the fundamental structural frequency of the robot. The value of G_2 was chosen based on impedance matching, while the values of G_1 ,G_3, and G_4 were chosen based on frequency domain analysis of Classical Control.

This controller is very robust. We did not introduce a model-sensitive compensator that would require a very accurate model of the system. Even if the velocity feedback around the base actuator is off by as much as 50% from the correct value, the system remains well behaved. Thus, Design in the Physical Domain led to a controller that is simple, yet robust as well.

IV. EXPERIMENTAL RESULTS

A five degree-of-freedom micromanipulator with the following specifications:

Degrees of freedom:	5 (3 in translation, 2 in rotation)
Payload:	50 pounds
Bandwidth:	50 Hz at maximum displacement
Maximum Displacement:	0.2 inches translation, 4°rotation
Size:	6 inch cube
Weight:	7.5 pounds (not including servo-valves)

was designed and fabricated (see Figure 14) The micromanipulator is controlled via hydraulic servo-valves and can accelerate a 22 Kg mass at 45G's.

There are 5 piston-pairs integrated into the package (one pair for each degree-of-freedom). Hence, all actuation is done through push-push action and not push-pull. This eliminates backlash. Furthermore, it allows for equal area on both sides of the pistons, which is beneficial for control. Each piston is one inch in diameter and can apply xxxx newtons (2300 lb) of force with an operating hydraulic pressure of xxxxkPa (3000 PSI). The force to weight ratio is 300:1. A more complete description of this prototype micromanipulator can be found in reference 2.

An experimental one-axis macro/micro manipulator test bed was designed and constructed. The micromanipulator described above was attached to a very flexible (first structural mode at 1.8 Hz), one-axis macromanipulator (see Figure 15). The reason for using such a flexible structure is to accentuate the stability problems by examining an extreme case. It is not meant to imply that robots should be constructed with floppy structures.

The macromanipulator is actuated at the base and can be controlled using either base measurements or endpoint (relative to ground) measurements. The micromanipu-

lator is controlled using only endpoint measurement. A number of experiments were performed in both endpoint position and force control. In both cases, the achieved performance of the macro/micro manipulator was compared to that of the macromanipulator alone.

A. Endpoint Position Control

In this experiment it was desired to control the position of the system endpoint. The micromanipulator was controlled using endpoint position and velocity feedback, while the macromanipulator was controlled using base position and velocity feedback. A step position command was simultaneously issued to both the macro and micro manipulators. The response of the system endpoint (micromanipulator position) as well as that of the macromanipulator is given in Figure 16a. It is seen how the micromanipulator reaches its target very quickly and locks in on it while the macromanipulator is still moving. Recall that there was no connection between the micromanipulator and ground. The micromanipulator was carried by the macromanipulator, yet it was capable of compensating for the macromanipulator's undesirable motion. The response of the macromanipulator alone (micromanipulator turned off) is given in Figure 16b for comparison purposes. The macro/micro manipulator settles in about 40 milliseconds while the macromanipulator settles in approximately 1.2 seconds. Thus, a macro/micro manipulator could greatly reduce cycle-time in a real application.

Figure 14. Prototype Micromanipulator.

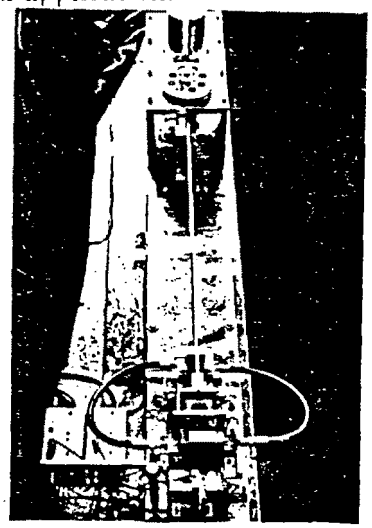

Figure 15. Experimental Macro/Micro Manipulator.

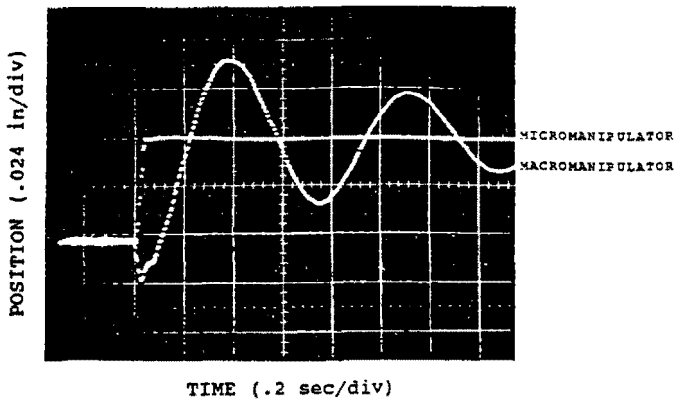

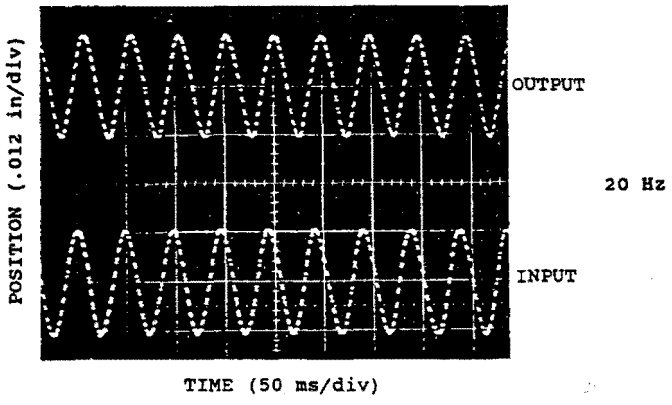

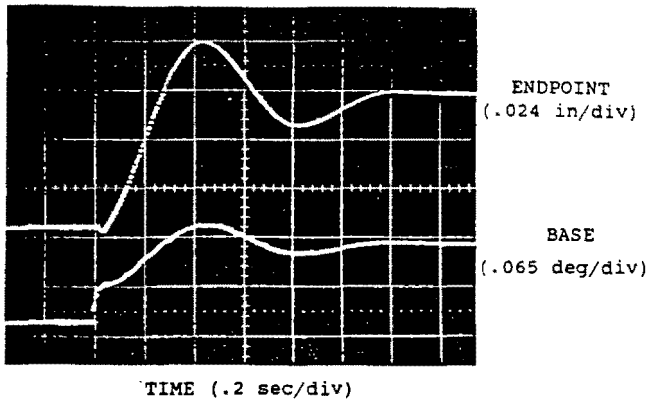

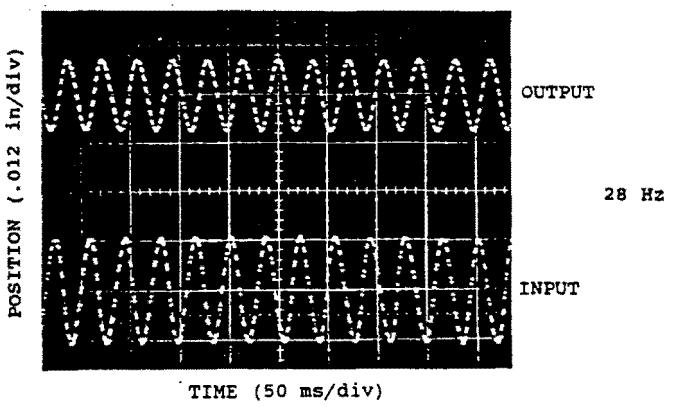

Figure 16. a. Response of Macro/Micro Manipulator to a Step Position Command
b. Response of Macromanipulator to a Step Position Command

Figure 17. Response of Macro/Micro Manipulator to Sinusoidal Position Commands

The micromanipulator was then issued a sinusoidal position command while the macromanipulator was regulated about zero. Figure 17 illustrates the response of the system endpoint vs input. At a frequencies upto 20 Hz the system tracks the input with no attenuation at all. A -3 dB bandwidth of 28 Hz was achieved. This is an order of magnitude higher than the first structural mode (1.8 Hz) and higher than the second structural mode (20 Hz) of the robot, confirming that a macro/micro manipulator architecture is inherently stable and well suited for endpoint position control.

B. High Bandwidth Force Control

It was desired, in this experiment, to control forces applied to an environment that is stiffer than the robot structure. A piezo-electric force transducer was attached to the endpoint of the system in order to measure the applied force. The stiffness of the environment was 15 lb/in, five times stiffer than the robot structure.

With the micromanipulator turned off, the macromanipulator was commanded to apply a force of 0.2 pounds to the environment. The force measurement from the transducer was fed back in a negative proportional fashion to the base motor. The initial position of the macromanipulator was 0.050 inches away from the environment. Hence, the system was out of contact with the environment at time zero. When the step force command was issued, the system impacted the environment and attempted to regulate the applied force. The force response at various gains is given in Figure 18. It is observed that as the gain was increased, bouncing became more severe. In fact, at a gain of about 2, the system became unstable. This confirms the analytical prediction that high performance force control on conventional robot architectures is inherently unstable due to non-collocation of actuator and sensor. Instability occurred despite the soft environment used. In fact, recent findings by Colgate [27] indicate that the stiffness of the environment relative to the robot structure is of primary importance, and not necessarily the absolute stiffness. More specifically, using conventional robot architectures, it is extremely difficult to achieve good force control against environments that are as stiff or stiffer than the robot structure.

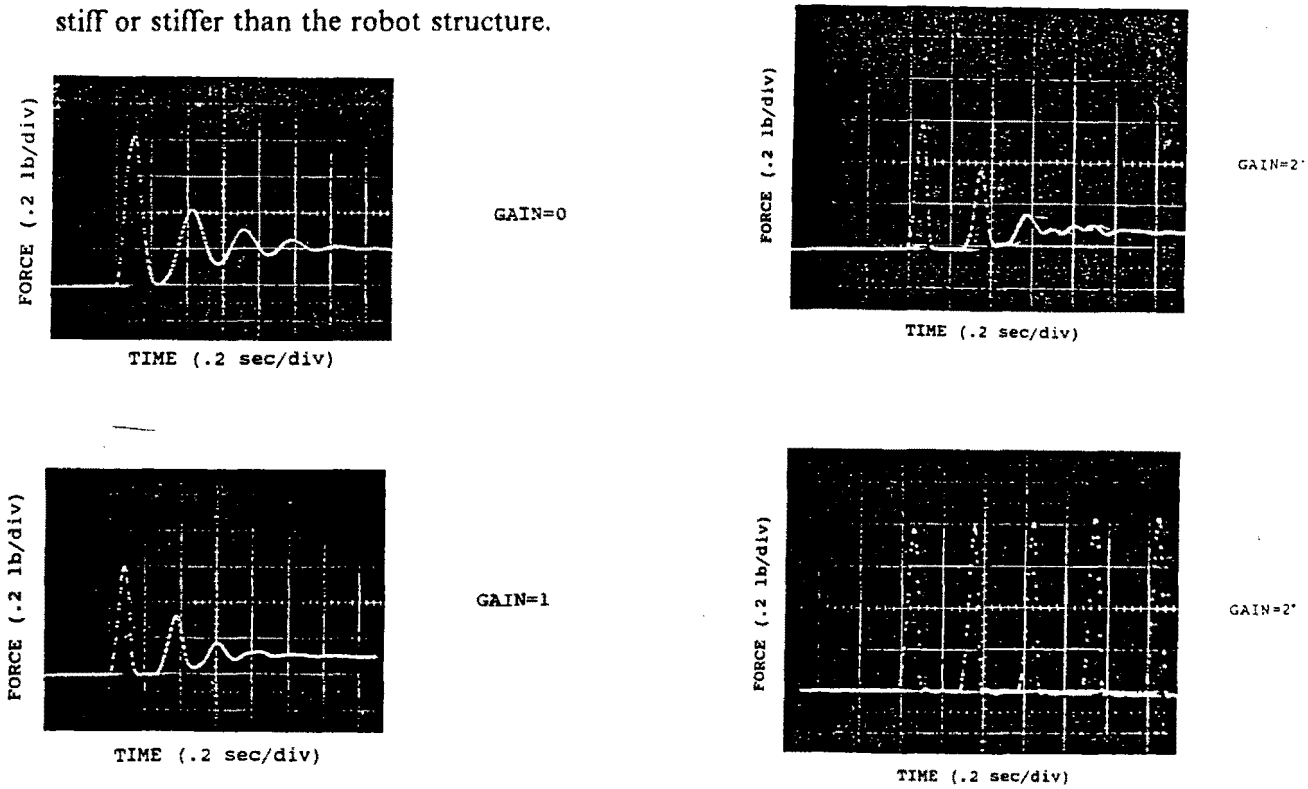

Figure 18. Response of Macromanipulator to a Step Force Command With Initial Impact.

In the next experiment, the micromanipulator was enabled and force was controlled by feeding back the measurement from the transducer to the micromanipulator in a negative proportional fashion. The macromanipulator was controlled about zero using base position and velocity feedback. Once again, the system began 0.050 inches away from the environment, giving rise to an impact. The force step response is shown in Figure 19a. The best obtained force control response of the macromanipulator alone (open loop) is repeated in Figure 19b for comparison purposes. It is seen in Figure 19a that the initial impact no longer produces a large force peak. Furthermore, the large oscillations exhibited by the macromanipulator are greatly suppressed.

Figure 20 illustrates the macro/micro manipulator's ability to track sinusoidal force commands. It is seen that up to a frequency of about 50 Hz there is virtually no attenuation. A -3 dB bandwidth of 60 Hz was obtained . This is 32 times higher than the first structural mode of the robot, demonstrating that a macro/micro manipulator is an inherently stable and well suited physical architecture for high bandwidth force control.

V. CONCLUSIONS

The macro/micro manipulator architecture was shown to be inherently stable and well suited for high performance endpoint control. The critical issue that had to be addressed is the dynamic coupling between the micromanipulator and macromanipulator

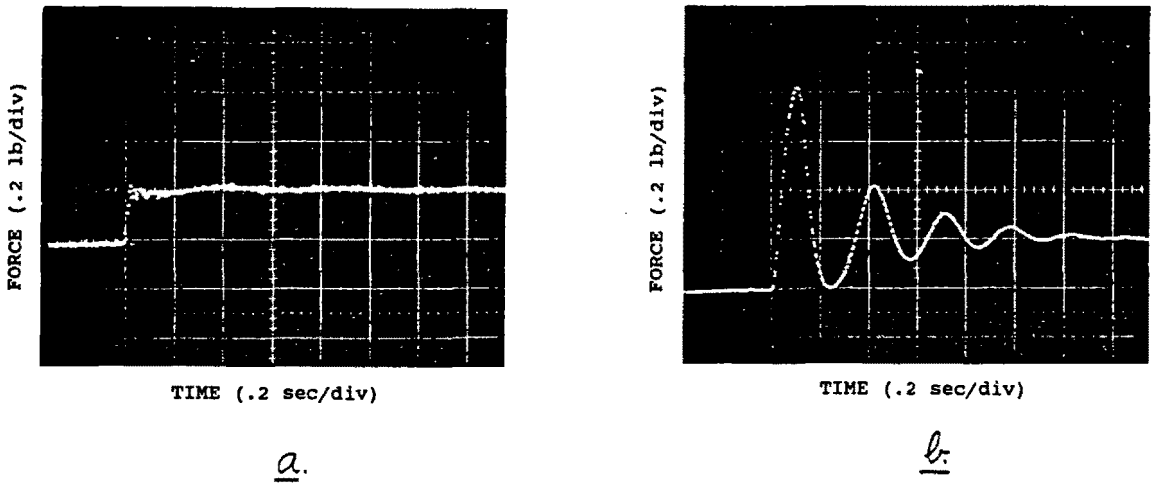

Figure 19. a. Response of Force Controlled Macro/Micro Manipulator to a Step Force Command With Initial Impact
b. Response of Macromanipulator to a Step Force Command With Initial Impact

structure. If the effective endpoint inertia of the macromanipulator is much greater than the inertia of the micromanipulator and load, then the dynamics of the macromanipulator can be neglected, and the system remains stable at all frequencies. In general, however, the dynamic coupling between the micromanipulator and macromanipulator leads to an instability band in the neighborhood of the structural frequency of the macromanipulator.

The proposed controller, designed in the physical domain, eliminates this problem. The controller is simple, yet robust. Its structure was not at all evident from the root locus and Bode plot of the system.

Both endpoint position and force control bandwidths higher than the fundamental structural frequency of the robot were achieved. This can improve accuracy, reduce cycle-time, and enhance the robot's capability to successfully interact with various environments.

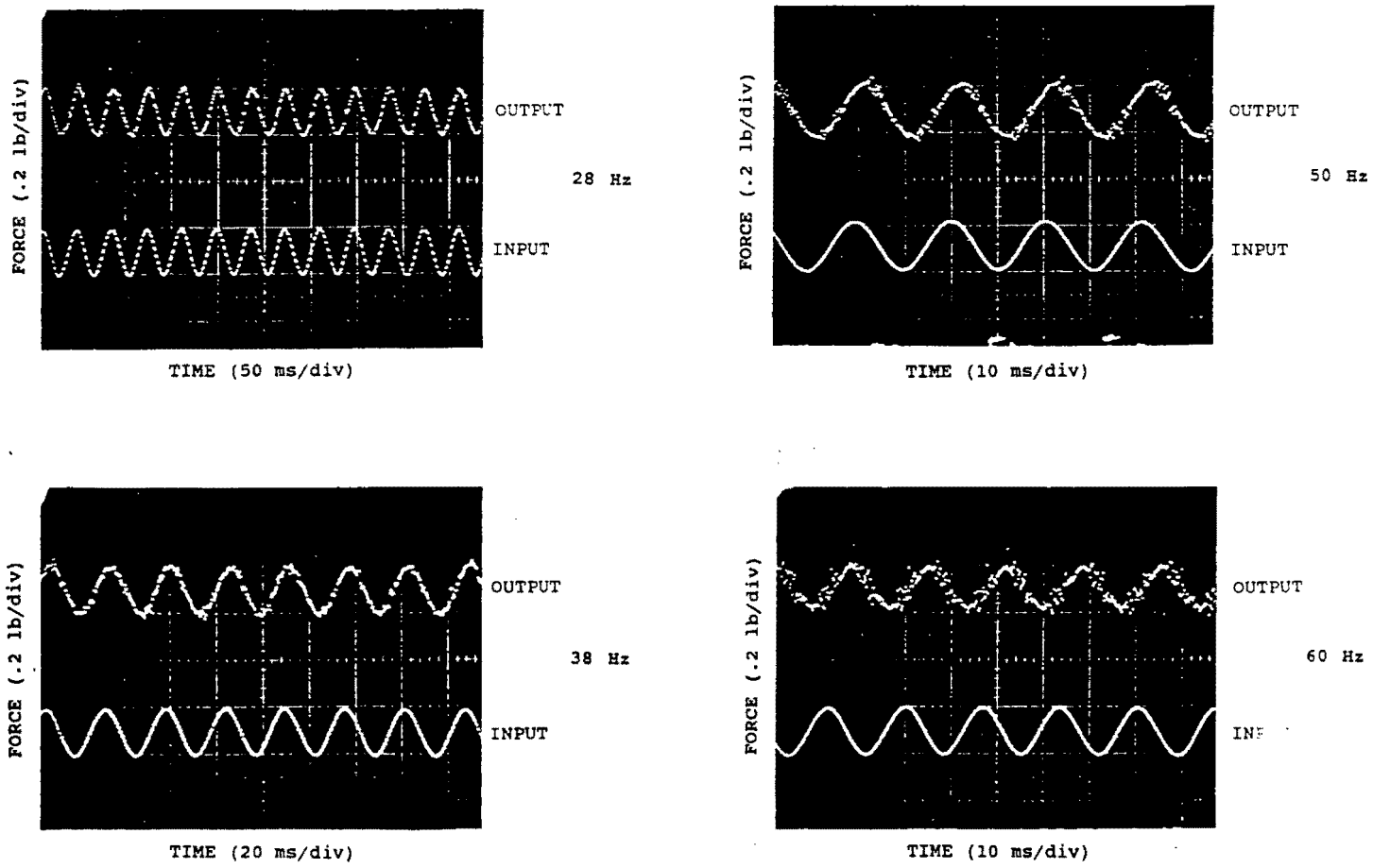

Figure 20. Response of Force Controlled Macro/Micro Manipulator to Sinusoidal Force Commands